Journal of Advanced Zoology
ISSN: 0253-7214
Volume ***44*** *Issue* ***S-2 Year 2023*** *Page* ***1885:1903***

Curcumin enriched nanoformulation: Characterization, solubility, stability and associated antioxidant, anti-inflammatory and anti-tyrosinase properties

Pooja Dalal[a] **and Rekha Rao**[a*]

[a] *Department of Pharmaceutical Sciences, Guru Jambheshwer University of Science & Technology, Hisar - 125001, Haryana, India*

***Corresponding author address:**
Rekha Rao
Department of Pharmaceutical Sciences, Guru Jambheshwar University of Science & Technology, Hisar - 125001, Haryana, India
E-mail address: rekhaline@gmail.com

Article History
Received: 12 August 2023
Revised: 10 September 2023
Accepted:10 October 2023

Abstract

curcumin (CUR), a natural bioactive, chiefly present in *Curcuma longa L.* rhizomes, exerts therapeutic potential for numerous chronic disorders by virtue of its profound anti-oxidant, anti-inflammatory and anti-tyrosinase action. Nonetheless, its therapeutic utility is hinders owing to its poor solubility, stability issues, fast metabolism, poor absorption and bioavailability issues. Polymer based nano systems have fascinated scientific community over the past few decades. As a potential polymer system, β-cyclodextrin nanosponges demonstrated the potential to entrap bioactives and aid in their solubility, stability and bioavailability. Hence, the current research work is aimed to formulate, characterize curcumin enriched nanosponges (CUR-NSs) and evaluate the anti-oxidant, anti-tyrosinase and anti-inflammatory activities. Initially, curcumin enriched nanosponges were fabricated by varying polymer: cross-linker ratios resulting in expectable entrapment, size and release profile. Besides successful characterization, solubility and photostability of CURNS4 were found enhanced in comparison to pure bioactive. Further, findings of anti-oxidant, anti-tyrosinase and anti-inflammatory activities were

found promising for CUR nanosponges. In vitro release of CUR was found enhanced in CURNS4 compared to pure bioactive. Hence, findings of this research work highlight the significance of CUR enriched nanosponges to appraise its effectiveness.

Keywords; Bioactive; β-cyclodextrin; Colloidal delivery system; Nanosponges, Polymer

1. Introduction

Currently, snowballing in epidemiologic and experimental reports demonstrated that plants and their derived products exhibit huge potential to prevent and treat various disorders (Manna et al., 2020). Plant products have been utilized as a folklore medicine since days of yore, which is directly linked to their promising medicinal properties and lower adverse effects in comparison to synthetic drugs (Anwar et al., 2021). In this context, curcumin (CUR), a natural bioactive, chiefly present in *Curcuma longa L.* rhizomes has a rich history of traditional usage in East Asian countries as a turmeric (curry powder) (Hafez Ghoran et al., 2022). This bioactive exerts therapeutic potential for numerous chronic disorders including neurodegenerative diseases, metabolic syndromes, arthritis, liver disorders, and in various cancers mainly by virtue of its profound anti-inflammatory and anti-oxidant action (Giordano and Tommonaro, 2019; Kah et al., 2023). However, CUR exhibit numerous challenges such as poor solubility, stability issues, fast metabolism, poor absorption and bioavailability issues, which hinders its utility (Iriventi et al., 2020).

To resolve the above-mentioned issues of CUR, selection of a suitable delivery system is very crucial. Nano-delivery systems demonstrated effective targeting, good pharmacokinetics, reduction in side-effects (Lalami et al., 2022). Polymer based nano systems have fascinated scientific community over the past few decades (Monfared et al., 2022). As a potential polymer system, β-cyclodextrin nanosponges aid in improvement of solubility, stability and bioavailability of the encased moieties (Kumar et al., 2019; Tejashri et al., 2013). NSs are hyper-crosslinked colloidal carriers which are biodegradable and possess good biocompatibility and low cytotoxicity to normal cells. Further, nanosponges have been widely employed as carrier

systems for various bioactives which helps in protecting the drug, enhance the stability and therapeutic potential of encased moieties (Gupta et al., 2021).

In view of the above-mentioned merits of nanosponges, the present study was designed to formulate and characterize curcumin enriched nanosponges and evaluate the effect of nanosponges on anti-oxidant, anti-tyrosinase and anti-inflammatory properties of curcumin.

2. Materials and Methods

2.1. Materials and Reagents

Curcumin was provided as gift sample by Sunpure Extract Pvt. Ltd., Delhi. β-cyclodextrin, mushroom tyrosinase, diphenyl carbonate, kojic acid, bovine serum albumin and 3-(4,5-dimethylthiazal-z-yl)-2,5-diphenylterazolium (MTT) were obtained from Sigma Aldrich, India. 2,2-diphenyl-1-picryl hydrazine (DPPH) was acquired from SpectroChem Pvt. Ltd., Mumbai, India. All other reagents and solvents used in this research were of analytical grade.

2.2. Preparation of CUR enriched Nanosponges

The five different molar proportions of β-CD and DPC i.e., 1:2, 1:4, 1:6, 1:8 and 1:10 were used for fabrication of nanosponges. In this green approach, both polymer and cross-linker were heated gradually without making use of any solvent. The mixture was continuously stirred during heating at constant temperature (6 hours) to allow reaction of both (β-CD and DPC). Subsequently, the obtained mixture was cool down to room temperature followed by washing with double distilled water to separate surplus β-CD. Thereafter, it was subjected to soxhlet extraction to expel out other impurities including phenol. The solid product (nanosponges) was dried at room temperature. To encapsulate bioactive, NSs were dispersed in distilled water with excess CUR and sonicated for 10 minutes followed by stirring for 24 hours. This solution was subjected to centrifugation (to isolate unreacted CUR) and filtered. Finally, lyophilization (at -20℃) was carried out to obtain final CUR loaded nanosponges (Nair et al., 2022).

2.2. Evaluation of Solubilization Potential of Nanosponges

Solubilization potential of CUR with different batches of nude nanosponges as well as β-CD was evaluated. For the same, excess quantity of bioactive was dispersed in 10 ml water. Thereafter, a

specific portion of nanosponges/polymer was added to above dispersion and agitated for overnight. The resultant solution was centrifuged and analyzed at λ_{max} 424 nm (Kumar and Rao, 2022).

2.3. Determination of Entrapment Efficiency, Particle Size and Zeta Potential

The nanosponge formulations were dispersed in methanol, followed by sonication. The obtained solutions were subjected to filtration and filtrate was diluted appropriately (Dora et al., 2016). Finally, absorbance was analyzed at 424 nm employing UV spectrometer. The encapsulation of CUR was calculated by using following formula:

$$\text{Drug Encapsulation Potential (\%)} = \frac{Actual\ amount\ of\ drug\ in\ nanoformulation}{Theoretical\ amount\ of\ drug\ in\ nanoformulation} \times 100 \quad (1)$$

The particle size analysis of CUR enriched nanosponges was carried out by employing Malvern Instrument, UK. The suspension of test samples was prepared in distilled water and evaluated for particle size and poly dispersity index (PDI). Same procedure was adopted for zeta potential measurement (Kadian et al., 2023).

2.4. Structural and Morphological Analysis

Structural and morphological analysis of nude NS4, CUR and CURNS4 was performed by fourier transform infrared spectrum (FTIR) (Perkin Elmer FTIR, Waltham, MA, USA; 4000 - 400 cm^{-1}), differential scanning calorimetry (DSC) (PerkinElmer Thermal Analyzer, USA; 0-350℃ temperature range), powder X-ray diffraction (P-XRD) (Rigaku Miniflex-II table top X-ray diffractometer; scanned at 2Θ angle between range 5°-80° under t25 mA and 40 kV), ^{1}H NMR (BRUKER Ascend^{TM} 400) and field emission scanning electron microscopy (FE-SEM) (JSM-7610FPlus, JOEL, Japan; gold coated) (Dalal and Rao, 2023).

2.5. Photostability study

Photostability was performed employing UVA lamp having wavelength range from 320–400 nm. The diluted solution (10 ml) of CUR and CURNS4 was kept under UV irradiation at a distance of 10 cm. At predetermined time intervals (over 1 hour), fixed amount of sample was taken out

and diluted with methanol to analyze under UV spectrometer (Anandam and Selvamuthukumar, 2014).

2.6. In Vitro Biological Activities

2.6.1. Anti-oxidant Assay

The DPPH assay is most widely employed in vitro assay to analyze the anti-oxidant activity of test samples. The DPPH• combine with anti-oxidant molecules, get reduced and color change was observed. The DPPH assay of CUR, CURNS4 and ascorbic acid (positive control) was performed according to method described by Fang and his research team (Fang et al., 2011). Various dilutions of samples were prepared (in methanol). Additionally, 0.1 mM solution of DPPH was prepared and kept in dark till further use. In 0.5 ml test sample1.5 ml DPPH solution was mixed and incubated at room temperature (for half hour). After incubation, absorbance was recorded at λ_{max} 515 nm. Absorbance for control sample was recorded with methanol. Antioxidant potential (%) was evaluated employing the formula given below:

$$\%\ Inhibition = [1 - \left(\frac{Sample\ absorbance}{Control\ absorbance}\right)] \times 100 \quad (2)$$

2.6.2. Anti-inflammatory Assay

The difference in anti-inflammatory potential of pure CUR and CURNS4 was evaluated with the help of protein denaturation assay employing bovine serum albumin. Bovine serum albumin (0.20 ml; 1%) solution was added in 2 ml of test samples (at different concentrations). The obtained solutions were incubated firstly, for 20 minutes at 37 °C, thereafter, heated for 5 min at 70 °C. After heating, solutions were cool down. Then, added phosphate buffer saline (7.4 pH; 2.80 ml) to each test sample. The control group was prepared without test samples. The turbidity of obtained solutions was measured spectrometrically at 660 nm (Marrelli et al., 2022). Protein denaturation inhibition (%) was calculated employing following equation:

$$\%\ Inhibition = [100 - \frac{Absorbance\ of\ sample - Absorbance\ of\ control}{Absorbance\ of\ control}] \times 100 \quad (3)$$

2.6.3. Anti-tyrosinase Assay

The anti-tyrosinase assay of CUR, CURNS4 and kojic acid (positive control) was done according to protocol mentioned by Gupta et al., with some adaptations (Gupta et al., 2021). For this assay, firstly, tyrosinase enzyme (10 µL) was added in mixture of phosphate buffer (pH 6.8; 50 mM) and different dilutions of test samples (10 µL). Thereafter, these samples were incubated (20 minutes; room temperature) and solution of L-dopa (20 µL) was mixed in each sample. After recording absorbance at 475 nm, tyrosinase inhibition (%) of samples were calculated employing given formula:

$$\% \ Tyrosinase \ Inhibition = [\frac{Absorbance \ of \ control - Absorbance \ of \ sample}{Absorbance \ of \ control}] \times 100 \quad (4)$$

2.7. In Vitro Release Assay

The in vitro release assay was performed for CUR and CURNS4 via dialysis method using phosphate buffer saline (PBS; pH 7.4) and methanol (1:1) as a release media. The samples were dispersed in release media (3 ml) in dialysis bag which was then immersed in beaker having release media (50 ml) at room temperature with continuous stirring (500 rpm; 24 hours). At fixed intervals, each sample (3 ml) was drawn out and restored with equivalent volume of fresh media (Nair et al., 2022). By using a UV-Visible spectrometer, the samples were examined at λ_{max} 424 nm. The release assay was performed in triplicate for each sample.

2.8. Statistical Analysis

All the experiments were analyzed thrice and experimental data was demonstrated as mean ± SD. Bonferroni post tests were employed for multiple comparisons with the help of GraphPad Prism 5.01 software.

3. Results and Discussion

3.1. Evaluation of Solubilization Potential of Nanosponges

Solubility of curcumin was examined in polymer and fabricated NSs (as shown in Fig. 1). The solubility of CUR was found maximum (18.23±0.15 µg/ml) in 1:4 ratio (CURNS4), followed by 1:6 (CURNS6) (12.43±2.52 µg/ml). The solubility of CUR was enhanced by four folds in NS4 compared to pure bioactive.

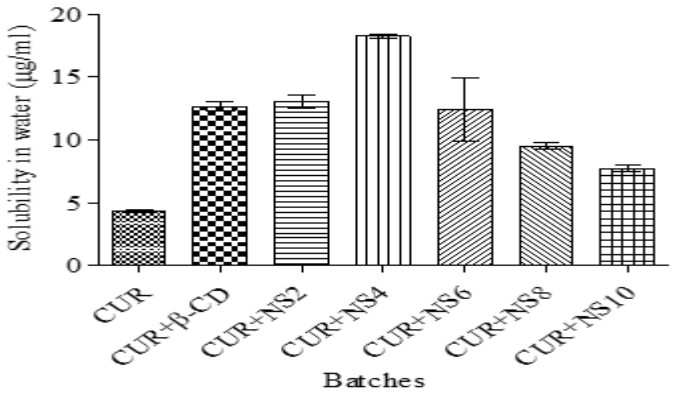

Fig. 1. Solubility study of CUR with β-CD and various prepared batches of nanosponges

3.2. Determination of Entrapment Efficiency, Particle Size and Zeta Potential

The entrapment efficiency of CURNS4 was obtained maximum i.e., 62.27 % ± 1.44 compared to other formulation batches (Fig. 2a). The particle size of formulations was found between 289 to 568.4 nm with desirable range of PDI. In case of CURNS4, the particle size was found minimum i.e. 289 nm with PDI 0.211 (Fig. 2b). Further, zeta potential was observed good from -21.0 to -25.5 and this was also found highest for CURNS4 (Fig. 2c).

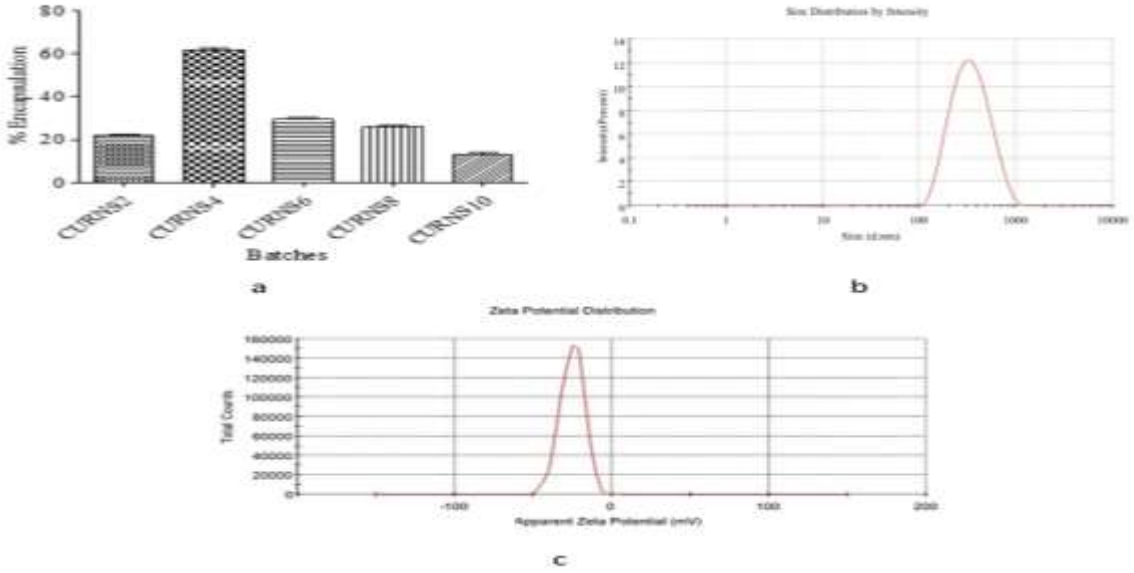

Fig. 2. Graphical representation of a) entrapment efficiency b) particle size and c) zeta potential of CUR loaded NS

On the basis of solubility, entrapment and particle size CURNS4 batch was chosen for further characterization and evaluation. The NS4 exhibited maximum solubility, encapsulation and smaller particle size. The porosity and cavity size of NSs are directly dependent on the number of functional groups and amount of cross-linker used. The cavities formed help in encapsulating the bioactives and modulate their crystallinity, which further leads to enhancement in their physical characteristics. Consequently, optimum ratio of polymer and cross-linker is required as it finally affects solubility, entrapment potential and solubilizing ability of the nanosponges (Omar et al., 2020). Further, molecular weight and structure of guest moiety also impact the polymer to drug ratio, which influence the particle size of nanosponge formulation (Jain et al., 2020). Hence, in some nanosponge formulations optimized batch is 1:4 (Kumar et al., 2021, 2018), whereas in others it is 1:6 (Kumar and Rao, 2020, 2021; Nair et al., 2022).

3.3. Structural and Morphological Analysis

FTIR spectra of CUR, CURNS4 and nude NS4 was assessed to get confirmation about bioactive enrichment into nanosponges (Fig. 3a). Firstly, FTIR spectrum of pure CUR was recorded to check its authentication. The spectrum exhibited characteristic peaks at 3511cm^{-1}, 1627 cm^{-1}, 1602 cm^{-1} , 1509 cm^{-1}, 1365 cm^{-1}, 1280 cm^{-1} and 1026 cm^{-1}, which were assigned to phenolic O–H stretching, C=C and C=O conjugation, stretching of the benzene ring, C=O vibration, -C-C stretching, enol C–O peak and C–O–C stretching, respectively (Rachmawati et al., 2013). Furthermore, spectrum of nude NS4 showed vibrational bands at 1774 cm^{-1}, 2933 cm^{-1}, 1419 cm^{-1} and 1029 cm^{-1} which were attributed to carbonate bond, C-H stretching, C-H bending and C-O stretching vibrations, respectively, supporting the synthesis of nude nanosponges. The CUR enrichment into NS4 was verified by the presence of almost similar wavenumbers as that of nude NS4 as well as signature peaks of native bioactive were either shifted, expanded or masked, which strengthened the evidence of bioactive loading. These results are in consistent with previously reported findings (Shah et al., 2019).

The thermal behavior of CUR, nude NS4 and CURNS4 was investigated by DSC (Fig.3b). The thermogram of CUR revealed a single sharp and clear endothermic peak at 175℃, corresponding to its melting point (Yadav and Kumar, 2014). The nude NS4 exhibited peak at around 56 °C; which was typically attributed to the release of water molecules. Further, no other endothermic

or exothermic peak was observed (Gharakhloo et al., 2020; Srivastava et al., 2021). With enrichment of CUR in nanosponges, peak of bioactive was shifted to 147℃ indicating its inclusion in nanosponges.

The data obtained from PXRD analysis of CUR, nude NS4 and CURNS4 is illustrated in Fig. 3c. The PXRD pattern of pure CUR showed strong and sharp diffraction peaks in 2θ region 12° to 29° indicating its crystalline nature (Peram et al., 2019). In contrast, intense peaks of bioactive either disappeared or their intensity was found reduced in PXRD of CUR enriched NS4 which might be attributed to its conversion to amorphous form (Srivastava et al., 2021). The intense and sharp peaks of nude NS4 were observed at 11.67°, 13.68°, 18.56°, 20.11°, 21.23°, 25.96°, and 29.11° highlighting formation of nanosponges.

^{1}H-NMR spectroscopy is a useful tool which offer quantitative evidences about the encapsulation of drug in nanoformulation. Fig. 3d shows the ^{1}H-NMR spectra of CUR, nude NS4 and CURNS4. The proton NMR spectrum of pure curcumin showed signals at 3.85, 6.07, 6.72, 6.81, 7.15, 7.33, 7.53 and 9.65 ppm (Singh et al., 2018). After enrichment in nanosponges, these signals were either disappeared or shifted revealing its encapsulation. Whereas, nude NS4 exhibited signals at 2.52, 3.64, 3.33, 4.45, 6.75, 7.40, 7.20, 7.90 and 9.32 ppm. Thus, all these findings from ^{1}H-NMR spectra advocated successful encapsulation as well as complexation of CUR in hydrophobic cavities of nanosponges.

FE-SEM photomicrographs of nude NS4 and CURNS4 were taken to assess the surface and morphological changes (Fig. 3e). The images depicted that nude nanosponges are nanoporous, spongy and spherical in shape. Whereas, FE-SEM image of CURNS4 revealed that porous structure of nude nanosponges were taken up with bioactive and ascertained its successful loading in the nanoporous formulation. The results of FE-SEM are interrelated with literature (Suvarna et al., 2021).

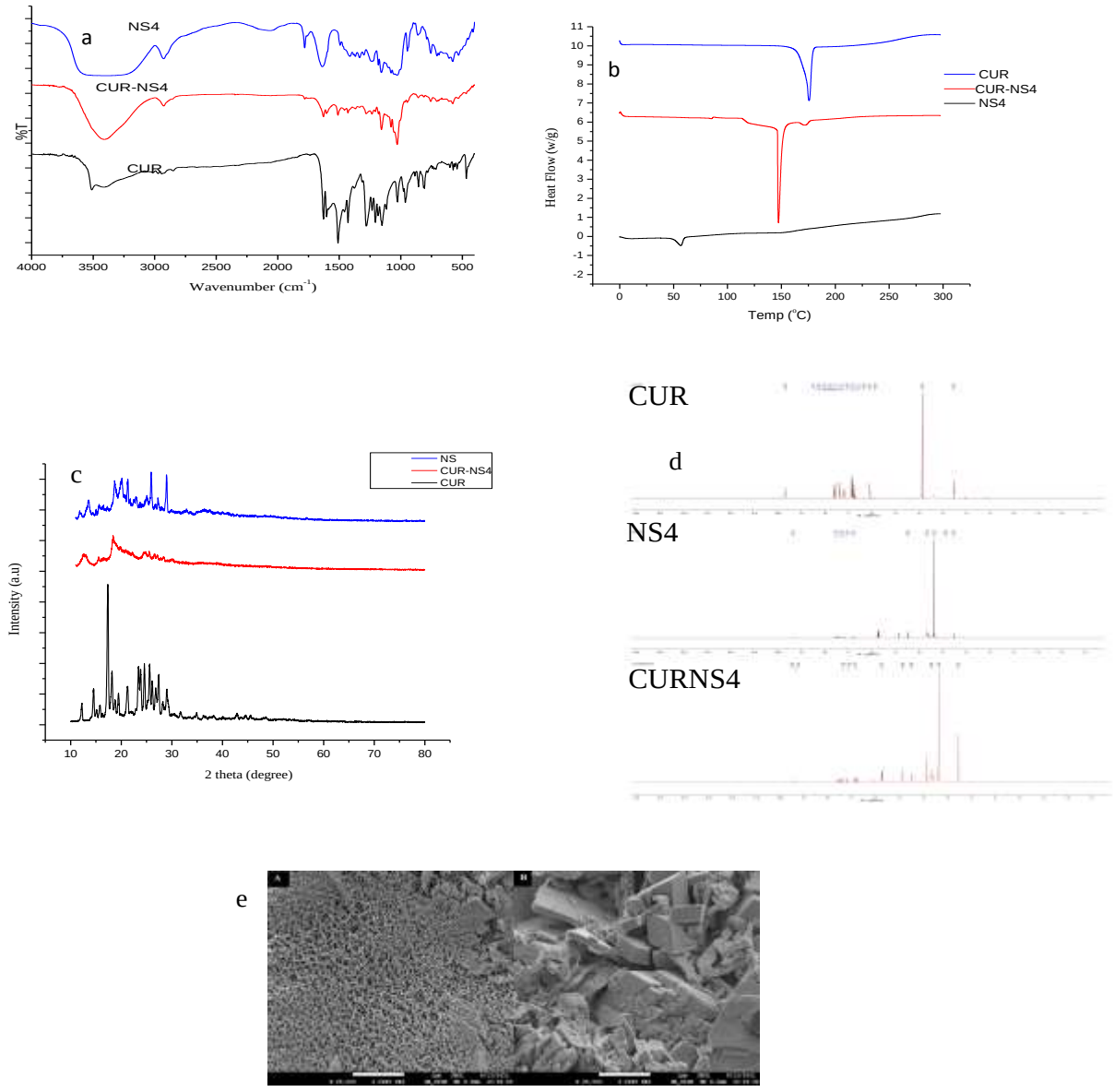

Fig. 3. Graphical representation of a) FTIR, b) DSC, c) P-XRD, d) H^1 NMR and e) FE-SEM of CUR, nude NS4 and CURNS4

3.4. Photostability study

This study was performed to investigate the effect of nanosponges on curcumin phostability and results are shown in Fig. 4. Percent drug residual for CUR and CURNS4 were found to be 33.58 ± 1.80 and 68.62 ± 2.77, respectively, after 1 hour of UV irradiation. Hence, results revealed that nanospnges exhibited improved photostability of bioactive after its encasement in NS.

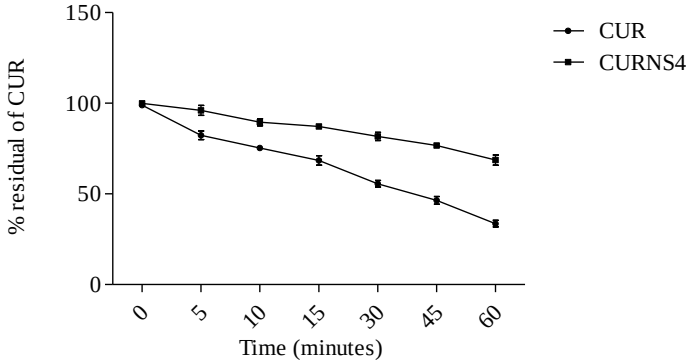

Fig. 4. Photodegradation of CUR and CURNS4

3.5. In Vitro Biological Activities

3.5.1. Anti-oxidant Assay

Our body exhibits various protective mechanisms against harmful free radicals and other reactive species. These free radicals are one of the key factors for etiology of various disorders. The anti-oxidants play a crucial role in suppressing excessive production of these free radicals (Sebastiammal et al., 2020). In this context, DPPH assay was employed to evaluate the scavenging potential of pure CUR, CURNS4 and ascorbic acid (as a standard) (Fig. 5). All the test samples at concentrations 10, 20, 50, 100, 200, 350 and 500 µg/ml tended to significantly boost anti-oxidant behavior which was found enhanced with increasing concentration. The results demonstrated that CUR enriched NS4 (79.12 % to 98.15 %) exhibited greater scavenging behavior in comparison to free form (74.72 % to 97.62 %) at all selected concentrations. The improved anti-oxidant capacity of CUR-NS4 confirmed improvement in bioactive solubility and its potential enrichment in nanoformulation architecture.

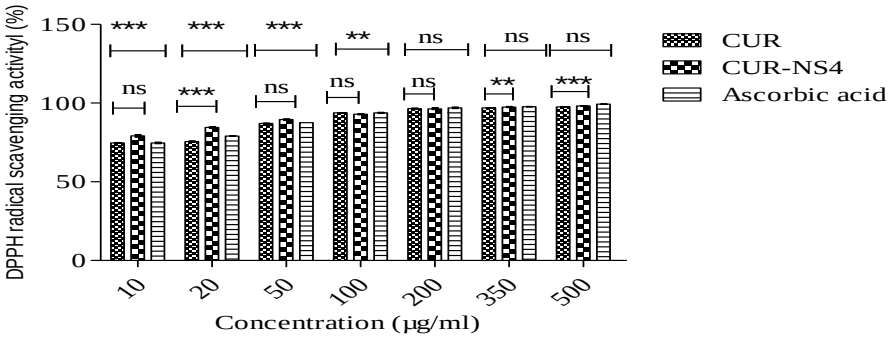

Fig. 5. Anti-oxidant potential of CUR, CURNS4 and Ascorbic acid at different concentrations

(n=3; ***p<0.001; **p<0.01 and ns is non-significant)

3.5.2. Anti-inflammatory Assay

Along with free radical generation, inflammation represents another hallmark associated with progression and development of various disorders (Diakos et al., 2014). On that account, bovine serum albumin denaturation assay was employed to evaluate the anti-inflammatory effect of CUR and CURNS4. Herein, outcomes point out that both samples exhibited concentration dependent anti-inflammatory effect. From results, it could be discerned that CURNS4 (69.54 % to 94.92 %) inhibited protein denaturation slightly better than pure CUR (68.18 % to 89.62 %), as it obvious in Fig. 6. The results of this assay were found in close agreement with anti-oxidant data (concentrations of samples were same in both studies).

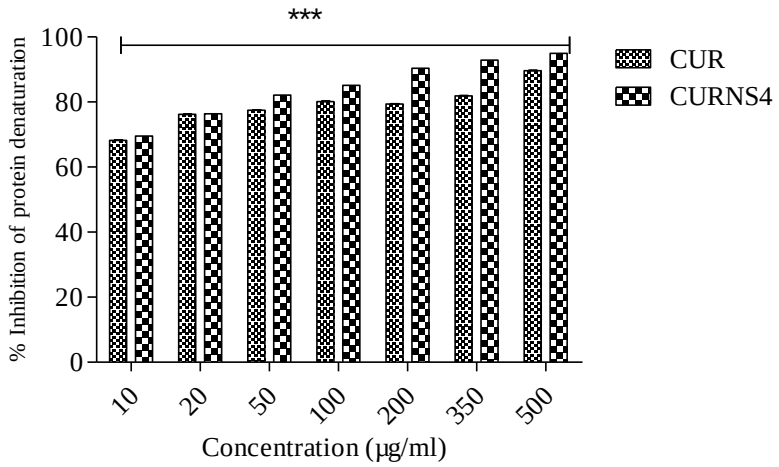

Fig. 6. Anti-inflammatory potential of CUR and CURNS4 at different concentrations (n=3; ***p<0.001)

3.5.3. Anti-tyrosinase Assay

The pharmaceutical and cosmetic industries are very interested in finding novel tyrosinase inhibitors due to their potential use in pigmentary diseases. (Harris et al., 2016). Hence, targeting this enzyme is an in-situ weapon for treatment of pigmentary disorders (Pu et al., 2020). Therefore, evaluation of anti-tyrosinase assay of nanoencapsulated bioactive is of vital significance in present investigation. Keeping this in view, herein, tyrosinase inhibition assay was performed for CUR, CURNS4 and kojic acid (as a standard). Tyrosinase inhibition of CUR, CURNS4 and kojic acid was found to be 92.26 %, 98.17 % and 98.19 %, respectively at highest

chosen concentration (Fig. 7). These results clearly depicted that enrichment of CUR in nanosponges significantly enhanced its anti-tyrosinase potential. It is worth mentioning here that results of CURNS4 were found almost near the standard i.e. kojic acid.

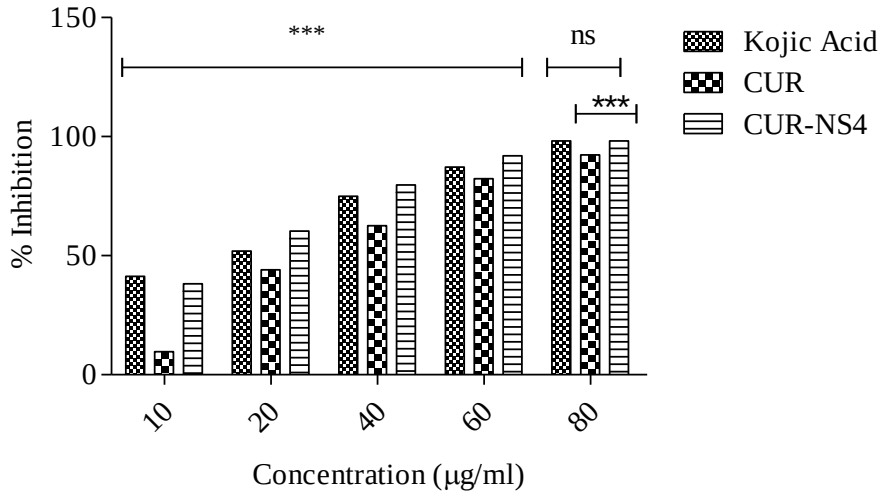

Fig. 7. Anti-tyrosinase potential of CUR, CURNS4 and Kojic acid at different concentrations (n=3; ***p<0.001and ns is non-significant)

3.6. In Vitro Release Assay

In vitro release of CUR and CURNS4 determines the release rate of bioactive at physiological pH conditions i.e., phosphate buffer saline (pH 7.4) (Fig. 14). A remarkable improvement in release profile of CUR was observed with CURNS4 than CUR alone. After, 24 hours, the cumulative release rate of CUR from NS4 was almost 90%, while only 59% of free bioactive was found released. These outcomes confirmed that curcumin enrichment into nanosponges significantly enhanced release profile of curcumin compared to free form. Herein, improvement in the release profile of CUR from CURNS4 may be ascribed owing to the various unique attributes of this nanosystem. Firstly, distribution of CUR in amorphous form in the cavities of nanosponges, secondly, enhancement in solubility of this poorly soluble bioactive, which might have promoted its fast dissolution and lastly, increase in surface area, owing to nano size formulation with porous structures. Nano size porous formulation further results in enhanced contact area and higher penetration of dissolution medium. All these features might have been responsible for augmented release of bioactive from nanosponges (Chilajwar et al., 2014; Mashaqbeh et al., 2021; Pushpalatha et al., 2019, 2018).

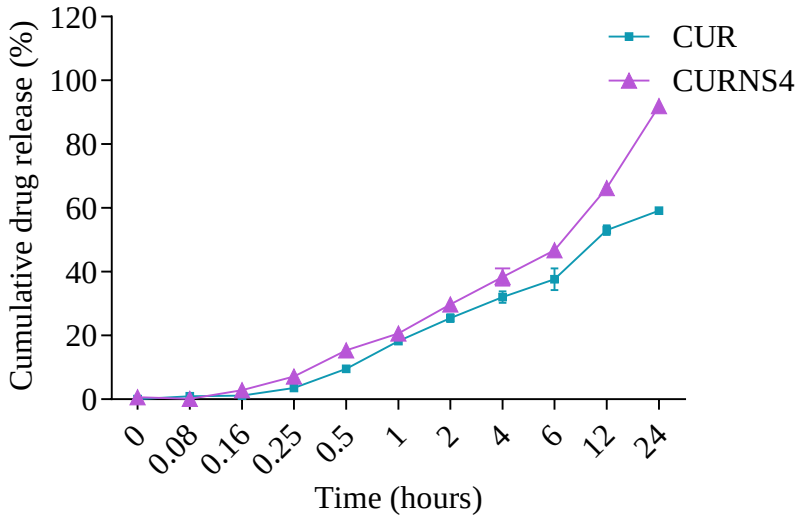

Fig. 14. In vitro release of CUR and CURNS4

4. Conclusion

In this study, curcumin enriched nanosponges were developed to enhance the therapeutic effectiveness of curcumin. Herein, different batches of CUR loaded NSs were successfully formulated and among them CURNS4 exhibited superior solubility, PSA and encapsulation, which was selected for further characterization and assessment. CURNS4 was found to significantly enhance various biological activities including anti-oxidant, anti-inflammatory and anti-tyrosinase when compared to pure CUR. Further, in vitro release demonstrated enhanced release profile of bioactive in CURNS4 compared to pure CUR. Taking all these aspects into consideration, it is suggested that CUR enrichment in nanosponge was found to be a promising strategy to enhance the functional properties of curcumin.

Author Contributions: Pooja Dalal: Conceptualization, Formal analysis, Investigation, Data curation, Writing – original draft, Visualization, Project administration. **Rekha Rao:** Formal analysis, Data curation, Writing – review & editing, Project administration.

Funding: This research work gets funding from ICMR-SRF, New Delhi (Grant no. 45/41/2020-NAN-BMS).

Declaration of interest: The authors declare no conflict of interest.

Acknowledgments: This research work was funded by Indian Council of Medical Research, Delhi, India for financial support (Grant no. 45/41/2020-NAN-BMS). Researchers also thanks Department of Pharmaceutical Sciences, Department of Food Technology and Dr. APJ Abdul kalam, central instrument laboratory of Guru Jambheshwar University of Science and Technology, Hisar (Haryana), India.

References

1. Anandam, S., Selvamuthukumar, S., 2014. Fabrication of cyclodextrin nanosponges for quercetin delivery: physicochemical characterization, photostability, and antioxidant effects. Journal of materials science 49, 8140–8153.
2. Anwar, D.M., El-Sayed, M., Reda, A., Fang, J.-Y., Khattab, S.N., Elzoghby, A.O., 2021. Recent advances in herbal combination nanomedicine for cancer: delivery technology and therapeutic outcomes. Expert opinion on drug delivery 18, 1609–1625.
3. Chilajwar, S.V., Pednekar, P.P., Jadhav, K.R., Gupta, G.J., Kadam, V.J., 2014. Cyclodextrin-based nanosponges: a propitious platform for enhancing drug delivery. Expert opinion on drug delivery 11, 111–120.
4. Dalal, P., Rao, R., 2023. β-cyclodextrin Nanosponges for Enhanced Anti-melanoma Potential of Silymarin with Functions of Anti-oxidant, Anti-inflammatory and Anti-tyrosinase. Results in Chemistry 101006.
5. Diakos, C.I., Charles, K.A., McMillan, D.C., Clarke, S.J., 2014. Cancer-related inflammation and treatment effectiveness. The Lancet Oncology 15, e493–e503.
6. Dora, C.P., Trotta, F., Kushwah, V., Devasari, N., Singh, C., Suresh, S., Jain, S., 2016. Potential of erlotinib cyclodextrin nanosponge complex to enhance solubility, dissolution rate, in vitro cytotoxicity and oral bioavailability. Carbohydrate polymers 137, 339–349.
7. Fang, R., Jing, H., Chai, Z., Zhao, G., Stoll, S., Ren, F., Liu, F., Leng, X., 2011. Design and characterization of protein-quercetin bioactive nanoparticles. Journal of nanobiotechnology 9, 1–14.
8. Gharakhloo, M., Sadjadi, S., Rezaeetabar, M., Askari, F., Rahimi, A., 2020. Cyclodextrin-Based Nanosponges for Improving Solubility and Sustainable Release of Curcumin. ChemistrySelect 5, 1734–1738.
9. Giordano, A., Tommonaro, G., 2019. Curcumin and cancer. Nutrients 11, 2376.

10. Gupta, B., Dalal, P., Rao, R., 2021. Cyclodextrin Decorated Nanosponges of Sesamol: Antioxidant, Anti-tyrosinase and Photostability Assessment. Food Bioscience 101098. https://doi.org/10.1016/j.fbio.2021.101098
11. Hafez Ghoran, S., Calcaterra, A., Abbasi, M., Taktaz, F., Nieselt, K., Babaei, E., 2022. Curcumin-based nanoformulations: A promising adjuvant towards cancer treatment. Molecules 27, 5236.
12. Harris, Z., Donovan, M.G., Branco, G.M., Limesand, K.H., Burd, R., 2016. Quercetin as an emerging anti-melanoma agent: a four-focus area therapeutic development strategy. Frontiers in nutrition 3, 48.
13. Iriventi, P., Gupta, N.V., Osmani, R.A.M., Balamuralidhara, V., 2020. Design & development of nanosponge loaded topical gel of curcumin and caffeine mixture for augmented treatment of psoriasis. DARU Journal of Pharmaceutical Sciences 28, 489–506.
14. Jain, A., Prajapati, S.K., Kumari, A., Mody, N., Bajpai, M., 2020. Engineered nanosponges as versatile biodegradable carriers: An insight. Journal of drug delivery science and technology 57, 101643.
15. Kadian, V., Dalal, P., Kumar, S., Kapoor, A., Rao, R., 2023. Comparative evaluation of dithranol-loaded nanosponges fabricated by solvent evaporation technique and melt method. Future Journal of Pharmaceutical Sciences 9, 1–15.
16. Kah, G., Chandran, R., Abrahamse, H., 2023. Curcumin a Natural Phenol and Its Therapeutic Role in Cancer and Photodynamic Therapy: A Review. Pharmaceutics 15, 639.
17. Kumar, A., Rao, R., 2022. Formulation and modification of physicochemical parameters of p-Coumaric acid by cyclodextrin nanosponges. Journal of Inclusion Phenomena and Macrocyclic Chemistry 1–14.
18. Kumar, A., Rao, R., 2020. Enhancing efficacy and safety of azelaic acid via encapsulation in cyclodextrin nanosponges: development, characterization and evaluation. Polymer Bulletin 1–28.
19. Kumar, S., Dalal, P., Rao, R., 2019. Cyclodextrin nanosponges: a promising approach for modulating drug delivery, in: Colloid Science in Pharmaceutical Nanotechnology. IntechOpen.

20. Kumar, S., Prasad, M., Rao, R., 2021. Topical delivery of clobetasol propionate loaded nanosponge hydrogel for effective treatment of psoriasis: Formulation, physicochemical characterization, antipsoriatic potential and biochemical estimation. Materials Science and Engineering: C 119, 111605.
21. Kumar, S., Rao, R., 2021. Novel Dithranol Loaded Cyclodextrin Nanosponges for Augmentation of Solubility, Photostability and Cytocompatibility. Current Nanoscience 17, 747–761.
22. Kumar, S., Trotta, F., Rao, R., 2018. Encapsulation of Babchi Oil in Cyclodextrin-Based Nanosponges: Physicochemical Characterization, Photodegradation, and In Vitro Cytotoxicity Studies. Pharmaceutics 10, 169.
23. Lalami, Z.A., Tafvizi, F., Naseh, V., Salehipour, M., 2022. Characterization and optimization of co-delivery Farnesol-Gingerol Niosomal formulation to enhance anticancer activities against breast cancer cells. Journal of Drug Delivery Science and Technology 72, 103371.
24. Manna, D., Akhtar, S., Maiti, P., Mondal, S., Kumar Mandal, T., Ghosh, R., 2020. Anticancer activity of a 1, 4-dihydropyridine in DMBA-induced mouse skin tumor model. Anti-Cancer Drugs 31, 394–402.
25. Marrelli, M., Amodeo, V., Puntillo, D., Statti, G., Conforti, F., 2022. In vitro antioxidant and anti-denaturation effects of Buglossoides purpurocaerulea (L.) IM Johnst. fruit extract. Natural Product Research 1–4.
26. Mashaqbeh, H., Obaidat, R., Al-Shar'i, N., 2021. Evaluation and characterization of curcumin-β-cyclodextrin and cyclodextrin-based nanosponge inclusion complexation. Polymers 13, 4073.
27. Monfared, Y.K., Mahmoudian, M., Caldera, F., Pedrazzo, A.R., Zakeri-Milani, P., Matencio, A., Trotta, F., 2022. Nisin delivery by nanosponges increases its anticancer activity against in-vivo melanoma model. Journal of Drug Delivery Science and Technology 104065.
28. Nair, A.B., Dalal, P., Kadian, V., Kumar, S., Kapoor, A., Garg, M., Rao, R., Aldhubiab, B., Sreeharsha, N., Almuqbil, R.M., 2022. Formulation, Characterization, Anti-Inflammatory and Cytotoxicity Study of Sesamol-Laden Nanosponges. Nanomaterials 12, 4211.

29. Omar, S.M., Ibrahim, F., Ismail, A., 2020. Formulation and Evaluation of Cyclodextrin-Based Nanosponges of Griseofulvin as Pediatric Oral Liquid Dosage Form for Enhancing Bioavailability and Masking Bitter Taste. Saudi Pharmaceutical Journal.
30. Peram, M.R., Jalalpure, S., Kumbar, V., Patil, S., Joshi, S., Bhat, K., Diwan, P., 2019. Factorial design based curcumin ethosomal nanocarriers for the skin cancer delivery: in vitro evaluation. Journal of liposome research 29, 291–311.
31. Pu, Y., Zhou, B., Xiang, H., Wu, W., Yin, H., Yue, W., Yin, Y., Li, H., Chen, Y., Xu, H., 2020. Tyrosinase-activated prodrug nanomedicine as oxidative stress amplifier for melanoma-specific treatment. Biomaterials 259, 120329.
32. Pushpalatha, R., Selvamuthukumar, S., Kilimozhi, D., 2019. Cyclodextrin nanosponge based hydrogel for the transdermal co-delivery of curcumin and resveratrol: Development, optimization, in vitro and ex vivo evaluation. Journal of Drug Delivery Science and Technology 52, 55–64.
33. Pushpalatha, R., Selvamuthukumar, S., Kilimozhi, D., 2018. Cross-linked, cyclodextrin-based nanosponges for curcumin delivery-physicochemical characterization, drug release, stability and cytotoxicity. Journal of Drug Delivery Science and Technology 45, 45–53.
34. Rachmawati, H., Edityaningrum, C.A., Mauludin, R., 2013. Molecular inclusion complex of curcumin–β-cyclodextrin nanoparticle to enhance curcumin skin permeability from hydrophilic matrix gel. Aaps Pharmscitech 14, 1303–1312.
35. Sebastiammal, S., Fathima, A.S.L., Devanesan, S., AlSalhi, M.S., Henry, J., Govindarajan, M., Vaseeharan, B., 2020. Curcumin-encased hydroxyapatite nanoparticles as novel biomaterials for antimicrobial, antioxidant and anticancer applications: A perspective of nano-based drug delivery. Journal of Drug Delivery Science and Technology 57, 101752.
36. Shah, N.V., Gohil, D.Y., Seth, A.K., Aundhia, C.J., Patel, S.S., 2019. Development of risedronate sodium-loaded nanosponges by experimental design: optimization and in vitro characterization. Indian Journal of Pharmaceutical Sciences 81, 309–316.
37. Singh, A.K., Yadav, S., Sharma, K., Firdaus, Z., Aditi, P., Neogi, K., Bansal, M., Gupta, M.K., Shanker, A., Singh, R.K., 2018. Quantum curcumin mediated inhibition of gingipains and mixed-biofilm of Porphyromonas gingivalis causing chronic periodontitis. RSC advances 8, 40426–40445.

38. Srivastava, S., Mahor, A., Singh, G., Bansal, K., Singh, P.P., Gupta, R., Dutt, R., Alanazi, A.M., Khan, A.A., Kesharwani, P., 2021. Formulation development, in vitro and in vivo evaluation of topical hydrogel formulation of econazole nitrate-loaded β-cyclodextrin nanosponges. Journal of Pharmaceutical Sciences 110, 3702–3714.
39. Suvarna, V., Singh, V., Sharma, D., Murahari, M., 2021. Experimental and computational insight of the supramolecular complexes of Irbesartan with β-cyclodextrin based nanosponges. Journal of Drug Delivery Science and Technology 63, 102494.
40. Tejashri, G., Amrita, B., Darshana, J., 2013. Cyclodextrin based nanosponges for pharmaceutical use: A review. Acta pharmaceutica 63, 335–358.
41. Yadav, D., Kumar, N., 2014. Nanonization of curcumin by antisolvent precipitation: process development, characterization, freeze drying and stability performance. International journal of pharmaceutics 477, 564–577.